



Published in final edited form as:

Obesity (Silver Spring). 2023 January ; 31(1): 159–170. doi:10.1002/oby.23583.

Effects of dietary methionine restriction on age-related changes in perivascular and beiging adipose tissues in the mouse

Marissa McGilvrey, BS^{*,1,3}, Bethany Fortier, BS^{*,1,2}, Benjamin Tero, BS¹, Diana Cooke, MS⁴, Emily Cooper, BS¹, Jeffrey Walker, PhD², Robert Koza, PhD^{1,3}, Gene Ables, PhD⁴, Lucy Liaw, PhD^{1,2,3}

¹Center for Molecular Medicine, MaineHealth Institute for Research

²Department of Biological Sciences, University of Southern Maine

³Graduate School of Biomedical Science and Engineering, University of Maine

⁴Orentreich Foundation for the Advancement of Science, Inc.

Abstract

Objective —Perivascular adipose tissue (PVAT) regulates vascular health. Dietary methionine restriction (MetR) impacts age-related adiposity, and we address its effects in PVAT.

Methods —Male C57BL/6 mice at 8, 52, and 102 weeks of age were fed standard (0.86%) or low methionine (0.12%) diets for 52 weeks in 8-week-old and 52-week-old mice, and for 15 weeks in 102-week-old mice.

Results —Mice with dietary MetR were resistant to weight gain and maintained a healthy blood profile. Aging increased lipid accumulation, and MetR reversed this phenotype. Notch signaling in inguinal white adipose tissue (iWAT), was decreased by MetR, but increased in gonadal WAT. However, the Notch phenotype of brown adipose tissue (BAT) was not affected by MetR. UCP-1 was increased in PVAT, iWAT and BAT by MetR when initiated in young mice, but this effect was lost in middle-aged mice.

Conclusions —Lipid in mouse PVAT peaks at 1 year of age, consistent with peak body mass. MetR reduced body weight, normalized metabolic parameters, and decreased lipid in PVAT in all age cohorts. Mice fed a MetR diet from early maturity to one year of age displayed an increased thermogenic adipocyte phenotype in iWAT PVAT, and BAT, all tissues with thermogenic capacity.

Keywords

methionine restriction; adipose; perivascular; aging

Corresponding author: Lucy Liaw PhD, Center for Molecular Medicine, MaineHealth Institute for Research, MaineHealth, 81 Research Drive, Scarborough, ME 04074, Tel 207-396-8142, Lucy.Liaw@mainehealth.org.

*M. McGilvrey and B. Fortier are co-first authors on this manuscript

Author contributions: MM, BF, BT, DC, RK, GA, and LL carried out experimentation and were involved in experimental design and interpretation. EC and JW participated in data analysis and interpretation. All authors were involved in the preparation of this manuscript, and approved the submitted version.

Disclosures - The authors declared no conflict of interest.

Introduction

Cardiovascular disease is a leading cause of mortality, with aging considered the critical risk factor¹. Dietary methionine restriction (MetR) has multiple anti-aging effects on adipose tissue, bone, liver, and the heart^{2–6}. In adipose tissue, MetR increases beigeing and reduces mitochondrial oxidative stress in multiple organs, including adipose tissue, leading to improved metabolic health and resistance to diet-induced obesity^{2, 3}. Some anti-obesity strategies target browning or beigeing mechanisms of adipose depots, which is reflective of increased mitochondrial abundance, lipid burning and thermogenic capacity, and has potential to protect from development of disease. Perivascular adipose tissue (PVAT) surrounds blood vessels and has a direct impact on vessel health and pathology. Studies in mouse models link the phenotype of PVAT with effects on vascular physiology⁷. One study observed that atherogenesis is enhanced by genetic loss of PVAT, and conversely atherogenesis is suppressed when thermogenesis of PVAT is induced by cold exposure⁸. While this suggests that PVAT functions as a crucial element controlling susceptibility to vascular disease, the molecular pathways mediating this are unclear. The effects of dietary MetR on PVAT anti-contractility have been explored⁹, however the effects on thermogenic and metabolic phenotypes of aortic PVAT have yet to be explored. Cellular and molecular changes in PVAT induced by dietary modification, such as high-fat diet and calorie restriction have been studied in mice. Mouse PVAT, specifically around the thoracic aorta, has characteristics of thermogenic adipocytes, similar to interscapular brown adipose tissue (BAT)^{10, 11}. We recently compared PVAT to brown and white adipose depots in mice and identified several novel protein signatures of thermogenic adipocytes, including glucose-related protein 75 (GRP75). We also identified Notch signaling as a regulator of PVAT phenotype¹². This was observed through elevated endogenous Notch signaling in PVAT with diet-induced obesity and was suppressed in PVAT with calorie restriction. Furthermore, constitutive activation of Notch signaling in adipose tissue was sufficient to initiate a whitening phenotype in PVAT, defined by increased lipid accumulation and suppression of thermogenic markers¹².

In this study, we characterized changes in PVAT due to normal aging in C57BL/6 mice in comparison to PVAT from mice with dietary MetR. Our results show that MetR prevents age-related weight gain and has a protective effect from whitening of PVAT in all three adult life phases of the mouse: young, middle-age, and old-age. Interestingly, this is similar to the effects of MetR in subcutaneous inguinal WAT, which has the ability to beige under conditions of cold or adrenergic stimulation^{13, 14}. The effects of MetR on PVAT have implications for development of cardiovascular disease, which is highly affected by a lean or obese whole-body phenotype and the thermogenic or lipid-storing features of PVAT.

Methods

See Supplemental Materials for expanded methods section.

Experimental Animals.

Studies were approved by the Institutional Animal Care and Use Committee of the Orentreich Foundation for the Advancement of Science. Male C57BL/6 mice were

purchased from Jackson Laboratory (Bar Harbor, ME). Mice were weight matched and separated into two groups, one for control diet composed of 14% kcal protein, 76% kcal carbohydrate, and 10% kcal fat (Research Diets, New Brunswick, NJ) with 0.86% methionine w/w, and the second with the same diet composition but with 0.12% methionine w/w. Diet composition is in Supplemental Table S1. Collectively, we examined the effects of MetR on the PVAT phenotype in three cohorts of mice. The cohorts were as follows: young mice were entered into the study at approximately 2 months (8 weeks) of age and consumed either control or MetR diet for 52 weeks (young, n=8/group), a second cohort of middle-aged mice at 12 months (52 weeks) of age were fed either control MetR diet for 52 weeks (middle, n=8/group), and a third cohort of old-aged mice at 23.5 months (102 weeks) of age were fed either control or MetR diet for 15 weeks (old, n= 5 for control diet and n=7 for MetR diet). These age groups were chosen to model different phases within the mature mouse lifespan: young adult, middle-aged adult, and old adult. These experimental groups are referred to based upon age of initiation of diet: young, middle, or old. Body weights were measured weekly and food consumption was measured biweekly. Mice were fasted prior to collection of plasma and tissues. Final body weights were determined, and liver weight measured. PVAT from young and middle-aged mice was collected from the thoracic aorta and fixed in formalin and paraffin embedded for sectioning. Other adipose tissues were flash frozen and stored at -80°C . We were limited by the size of PVAT and were unable obtain sufficient protein for immunoblot. This study was performed in male mice, and thus does not address potential sex differences in responses to methionine restriction. Previous experiments have shown that there is sexual dimorphism in phenotype depending on the initiation of age of the dietary intervention¹⁵. With MetR initiated in young mice at 8 weeks of age, males are responsive with loss of body weight and decreased adipose tissue expansion. Female mice, on the other hand, when initiated with MetR at 8 weeks of age, do not have changes in adipose tissue, but rather have loss of lean mass. Because of our focus on adiposity and the thermogenic phenotype of adipocytes, we chose to focus on male mice due to the documented overall change in adiposity due to MetR¹⁵.

Plasma Biochemical Analysis—Enzyme-linked immunosorbent assays were used to quantify plasma adiponectin, insulin-like growth factor 1 (IGF1), leptin (R&D Systems, Minneapolis MN), insulin (ALPCO Diagnostics, Salem NH), and FGF21 (Millipore, Billerica MA). Blood glucose was measured from a tail nick using a FreeStyle glucometer and test strips (Abbott, Chicago IL).

Histological Analysis—PVAT was fixed in 10% formalin (ThermoFisher), paraffin embedded, and sectioned at $5\mu\text{m}$ and stained with hematoxylin/eosin. Lipid quantification was performed as previously published¹⁶ using ImageJ software (NIH, Bethesda MD). Two raters performed quantification, and average results are reported as percent lipid area out of total PVAT area.

Immunostaining and Microscopy—For immunofluorescence staining, slides were deparaffinized, followed by heated antigen retrieval (0.01M sodium citrate buffer pH 6.0) for 25 minute, and permeabilization (TBS + 0.1% Triton-X) for 10 minutes. Sections were blocked in TBS with 5% goat serum and 1% BSA and for 2 hours. For mouse monoclonal

antibodies, sections were incubated with M.O.M.[®] Blocking Reagent (Vector Laboratories, Burlingame, CA) for 30 minutes then washed. Primary antibodies were incubated in TBS supplemented with 1% BSA and 0.1% Tween overnight at 4°C, washed with TBS-T. For immunofluorescence, samples were incubated with Alexa Fluor-conjugated secondary antibody in 1% BSA/TBS-T for 2h. Sections were washed, incubated with TrueVIEW[®] Autofluorescence Quenching Kit (Vector Laboratories) for 2 minutes. After washing, slides were coverslipped using Vectashield[®] Hard Set Antifade mounting medium with DAPI (Vector Laboratories). Images were captured using a Leica TCS SP8 confocal microscope, and fluorescence quantified with ImageJ. The baseline of tissue fluorescence was controlled for using IgG isotype antibody, and this value was subtracted. For TOM20 immunostaining, slides were deparaffinized, followed by heated antigen retrieval (0.01M sodium citrate buffer pH 6.0) for 30 minutes. Sections were blocked in PBS with 5% goat serum and 1% BSA and for 1 hour, and primary antibody was incubated in PBS supplemented with 1% BSA and 0.1% Tween overnight at 4°C. Sections were with PBS-T and incubated with Avidin/Biotin Blocking solution (Vector Laboratories, #SP-2001). Samples were then incubated with biotinylated secondary antibody for 2 hours (Jackson ImmunoResearch). Slides were incubation with Avidin/Biotinylated Conjugated Enzyme Peroxidase System (ABC Elite, Vector Laboratories, #PK-6100). Sections were reacted with diaminobenzidine for 5 mins, quenched and counterstained with hematoxylin nuclear stain, and coverslipped using Permount mounting medium (Fisher Scientific, #SP15). Additional information on antibodies is provided in Supplemental Data, Table S2.

Protein Isolation and Immunoblotting—Adipose tissues were lysed mechanically with a tube pestle in RIPA buffer (150 mM NaCl, 2mM EDTA, 1% Igepal, 0.5% sodium deoxycholate, 0.1% sodium dodecyl sulfate, and 50mM Tris HCl pH=7.4) with 1x protease/phosphatase inhibitor cocktail (Cell Signaling, Danvers MA) on ice. Lysates were sonicated and centrifuged at 11000g for 10 minutes at 4°C. Proteins were precipitated using 4 volumes ice cold 100% acetone, and incubation at -20°C overnight. Proteins were pelleted by centrifugation at 10000g for 10 minutes at 4°C, washed 2 times in 70% acetone and air dried. Pellets were resuspended in RIPA supplemented to 1% SDS with 1x protease/phosphatase inhibitor cocktail (Cell Signaling), sonicated, and stored at -20°C. Protein was quantified using the BioRad (Hercules, CA) DC protein assay, put in Laemmli sample buffer with 100 mM DTT, and incubated at 95°C for 15 minutes. SDS-PAGE was performed using BioRad TGX FastCast gels between 10% and 12% (1610173, 1610175) and 45–50µg protein/lane. Gels were transferred to PVDF membranes and blocked using 5% milk/0.1% Tween in PBS. Primary antibodies were diluted in 5% milk and incubated overnight at 4°C. Signal was detected using Luminata[™] Classico or Forte Western HRP Substrates (Millipore, Billerica MA). Additional information is provided in Supplemental Table S2. Mouse PVAT is very limited in comparison to all other adipose depots in the mouse, and thus we were unable to perform immunoblot on PVAT due to small tissue size.

Statistical Analysis—Data are presented as means ± SEM. Comparisons within control and experimental diet groups were conducted using unpaired *t* tests for end point analyses. Comparisons between age groups were conducted using one-way analysis of variance (ANOVA). Differences were considered significant at $p < 0.05$. Statistical analysis was

performed in PRISM software version 8.4.3 (GraphPad Software, La Jolla, California). Differences in tissue mass were calculated using ANCOVA with body weight as covariate using R (version 3.6.1) and R Studio (version 1.2.1135).

Results

Dietary MetR improves physiologic measures of health during aging

To determine the effects of a MetR diet on physiologic factors that correlate with PVAT phenotype during different age phases, we studied three cohorts of C57BL/6 male mice fed a standard 0.86% methionine chow diet (control) or a 0.12% methionine restricted (MetR) diet. We modeled the experiment to represent young, middle-aged, and old mice. The first cohort of mice (young) initiated diet at 8 weeks (2 months) of age for a duration of 52 weeks; the middle-aged cohort (middle) initiated diet at 52 weeks (12 months) of age for a duration of 52 weeks; and the old cohort (old) initiated diet at 102 weeks (23.5 months) of age for a duration of 15 weeks. Within the first year of life, mice on control diet steadily gained weight up to 40 weeks of age, and then plateaued until 60 weeks of age (Fig 1A, Young). MetR reduced body weight significantly compared to controls ($p < 0.05$) in the young cohort after 3 weeks of MetR, which persisted to the end of one year. Middle aged mice at 52 weeks of age have significantly higher body weight compared to 8 week old mice. In the middle-aged mice with dietary intervention starting at 52 weeks of age, there was a significant difference in body starting at 2 weeks of MetR diet, compared to the control diet (Fig. 1A, Middle). The starting body weight of mice at 102 weeks of age was also significantly greater than the middle aged mice at 52 weeks of age. For this oldest cohort of mice, those on the MetR diet had significantly lower weight than their controls after 3 weeks of dietary intervention. Significant weight loss with MetR occurred at all age phases despite mice consuming significantly more of the MetR diet than the control diet in relation to their body weight (food/BW, Fig. 1B), demonstrating that these mice are not calorie deficient. In all age cohorts, MetR significantly reduced weight gain regardless of the age at which MetR diet was initiated (Fig. 1C). In addition, proportional liver weights were significantly decreased by MetR compared to its age-matched control (Fig. 1D).

Terminal plasma analysis revealed that MetR mice displayed a more metabolically healthy profile compared to controls. There were significant reductions in glucose, insulin, leptin and IGF-1 in MetR diet groups (Fig. 1E–H), which is in agreement with previous findings^{5, 17, 18}. Circulating adiponectin and FGF21 concentrations were significantly higher in MetR mice compared to controls (Fig. 1I–J). Previous studies in rodents demonstrated an impact of MetR on other adipose depots as well as the liver^{3, 19–21}. Thus we examined whether MetR in this aging study altered total mass of white adipose depots, liver, and skeletal muscle. Upon ANCOVA adjustment for body weight, MetR mice show no significant difference in the mass of gonadal white adipose tissue (gWAT), muscle, or liver in comparison to controls (Supplemental Fig. S1). However, when we compare liver weight at as percentage relative to body weight, we have significant differences between control and MetR in all three age groups (Fig 1D).

Effects of MetR on PVAT in mice at different ages

During the normal aging process, C57BL/6 mice on a regular chow diet gain weight, although they do not reach the level of obesity that can be induced by high-fat feeding. Likewise, while high-fat diet has been used to study lipid accumulation and adipose expansion, including in PVAT²², normal aging also increases lipid accumulation, albeit to a lower extent than obesity. We previously reported that lipid proportion within PVAT of C57BL/6 mice fed a standard chow diet at 12–14 weeks of age ranged from ~50–56%²², and we found higher lipid deposition in PVAT from one year old mice (Fig. 2A, C, Young), with a range from ~57–62%. In the comparable aged MetR group with the dietary intervention started in young mice, the lipid content was significantly decreased (Fig. 2B–C), with a range from ~35–43%. Similarly, in the middle and old age groups, there were also significantly lower proportions of lipid in the MetR groups compared to their respective controls. Interesting, there were no statistically significant differences in the lipid proportion in control fed mice across the age cohorts or the MetR groups across the age cohorts (Fig. 2D). Since lipid turnover can be associated with mitochondrial activity, we localized translocase of outer mitochondrial membrane 20 (TOM20) by immunostaining to detect mitochondria. Along with the decrease in lipid accumulation in PVAT, young adult mice fed a MetR diet had elevated TOM20 protein within PVAT (Fig. 2E). In the cohort of mice with diet initiated in middle age, TOM20 was present in both control and MetR diet, with no apparent difference in levels (Fig. 2F). Compared to the young cohort with MetR diet, the middle-aged cohort on MetR diet had lower TOM20 protein.

Lower lipid content and elevated TOM20 with MetR restriction suggested that the PVAT was adopting a more thermogenic phenotype. This phenotype can be described with lower lipid and increased markers of thermogenesis, including mitochondrial proteins. In the young cohort, PVAT from the MetR group was associated with elevated uncoupling protein 1 (UCP1), cytochrome c oxidase subunit IV (CoxIV), and GRP75, which was previously identified by our lab as a novel marker of thermogenic adipocytes¹² (Fig. 3A, C). Levels of perilipin1 (PLIN1), a lipid droplet surface marker, and PGC1 α , a transcriptional regulator of metabolism and mitochondrial biogenesis, were decreased after MetR in the young cohort of mice at 60 weeks of age. These data indicate that MetR counteracts the whitening process of PVAT due to aging and supports the maintenance of the thermogenic state when the diet is initiated in young adult mice (8 weeks of age) and maintained up to one year of age. Interestingly, this difference was not found in the middle-aged cohorts. These mice, despite having low lipid proportions, had lower levels of UCP1, CoxIV, and GRP85 compared to their respective controls (Fig. 3B, C).

Methionine restriction affects beiging adipose depots during aging

We next performed analysis of other adipose depots, including those that are able to beige, or increase thermogenesis. The ability of white adipose tissue (WAT) to undergo a beiging process to increase thermogenesis is a feature of particular depots, including subcutaneous inguinal WAT (iWAT) and retroperitoneal WAT (rpWAT)¹⁴ (Fig. 4). Thus, we assessed changes in both depots with aging on a control or MetR diet to understand if these depots were regulated similarly to PVAT. We utilized the young cohort that were fed the diet until 60 weeks of age. Immunoblot of iWAT (Fig. 5A–B) showed a 9-fold increase in levels

of the thermogenic marker UCP1 and a 3.5-fold increase in levels of CoxIV in the MetR mice compared to control, indicative of a metabolically healthy phenotype in a depot able to undergo the process of beiging²³. With the previous identification by our lab of the ability of Notch signaling pathway activation to induce a whitening phenotype in PVAT¹², it was further explored in these depots. Members of this pathway, Notch1 and HES5, were 70% and 28% lower, respectively, in the MetR mouse iWAT compared to controls. PLIN1 was present at 50% of control levels ($p < 0.05$), representative of a reduction in adiposity common with MetR and disruption of lipogenic / lipolytic balance. In rpWAT (Fig. 5C–D), we found a similar trend with Notch signaling proteins. Notch2 was 79% lower in the MetR group ($p < 0.0001$), and though Notch1 and HES5 were lower compared to controls (29% and 32%, respectively), this was not statistically significant. In alignment with the response in iWAT, PLIN1 was significantly lower in rpWAT from MetR mice compared to controls ($p < 0.0001$). Moreover, Cluster of Differentiation 68 (CD68), often used as an inflammation marker associated with the involvement of monocytes/macrophages, was significantly lower in rpWAT in mice fed a MetR diet ($p < 0.0001$).

Methionine restriction exhibits depot-specific effects

To complete our analysis of how MetR affects diverse adipose tissues, we analyzed interscapular brown adipose tissue (BAT) and gonadal white adipose tissue (gWAT, Fig. 4), which are commonly recognized as exhibiting opposite phenotypes and contribution to pathology. Mouse thoracic PVAT, though distinct from BAT or gWAT, has more characteristics of BAT and in health, influences vascular tone and function. We examined several markers associated with a metabolically healthy, thermogenic profile (Fig. 6A–B). Peroxisome proliferator-activated receptor gamma coactivator 1-alpha (PGC1 α), considered the master regulator of mitochondrial biogenesis, demonstrated no significant difference in MetR mouse BAT compared to controls. In stark contrast, PGC1 α was not detectable in gWAT samples processed synchronously with BAT. CoxIV, the terminal enzyme of the mitochondrial electron transport chain and inner mitochondrial membrane marker, demonstrated depot-specific expression similar to PGC1 α . There was no significant difference in MetR mouse BAT or gWAT compared to their respective controls, however CoxIV levels were negligible in gWAT samples in comparison to BAT. In contrast, UCP1 demonstrated a significant increase ($p < 0.0163$) in BAT of mice fed a MetR diet when compared to controls, and as with PGC1 α , was similarly absent in all gWAT samples. GRP75 increased by 25% in MetR mice though did not reach statistical significance ($p < 0.066$) in comparison to control. Conversely, GRP75 expression was 35% less than control in MetR mouse gWAT (Fig. 6B).

To observe the effect of MetR on the dichotomous phenotypes of adipose tissue, we examined several markers involved in the regulation of adipogenesis (Fig. 6C–D). Peroxisome proliferator activated receptor gamma (PPAR γ) is a master regulator of adipogenesis that has been shown to increase insulin sensitivity in part through enhanced release of adiponectin from adipose cells. BAT from MetR mice demonstrated a 26% increase in PPAR γ over controls but did not reach statistical significance. In gWAT, PPAR γ levels showed no statistical difference between the control and MetR mice, but were 3% lower than the MetR BAT mice (Fig. 6D). CCAAT/enhancer binding protein

alpha (C/EBP α), recognized along with PPAR γ as an important early regulator in adipogenesis^{24, 25}, is 33% lower in the BAT of MetR mice, a significant decrease ($p < 0.0155$) when compared to controls. In contrast, C/EBP α trended upward in the gWAT of mice on MetR diet, though not statistically significant. PLIN1, which is responsive to the metabolic status of mature adipocytes²⁶, shows a significant reduction ($p < 0.0485$) in BAT of mice on the MetR diet, with a loss of 27% when compared to controls. Although a downward trend is seen in the gWAT of MetR mice compared to controls with a loss of 16%, it does not reach statistical significance. Of note, levels of PLIN1 in BAT are higher in both control and MetR in comparison to gWAT. Fatty acid binding protein 4 (FABP4), which is involved in the formation of mature adipocytes and has important roles in the development of insulin resistance and atherosclerosis^{24, 27}, showed no significant difference with MetR for either BAT or gWAT compared to control, but demonstrated substantial differences between depots for both groups (Fig. 6D).

We also examined markers associated with the inflammatory phenotype of PVAT that are positively correlated with body mass, as well as the Notch signaling pathway previously mentioned (Fig. 6E–F). Both Notch1 and Notch2 levels in BAT from mice on a MetR diet were significantly less than controls, at 42% ($p < 0.0140$) and 37% ($p < 0.0089$) respectively. Interestingly, the opposite effect was seen in gWAT, with Notch1 demonstrating a significant 4-fold increase ($p < 0.038$) with MetR compared to controls and Notch 2 trending upward with a 1.8-fold increase which was not statistically significant ($p < 0.1340$). Despite not reaching significance, transcription factor and downstream Notch signaling pathway member, HES5, slightly increased in both BAT and gWAT with MetR (6% and 4% respectively) when compared to controls in alignment with Notch1 and 2 results. Levels of all Notch signaling pathway members were consistently higher in gWAT when compared to BAT, indicative of a depot-specific response. Cluster of differentiation molecule 11b (CD11b), also known as Mac-1, integrin alpha M (ITGAM), and complement receptor (CR3), is frequently used as a macrophage marker and indicator of inflammation²⁸. The gWAT of mice fed a MetR diet showed a significant decrease of 65% ($p < 0.0014$) in CD11b when compared to control. In contrast, levels of CD11b were undetectable in either control or MetR BAT (Fig. 6F).

Discussion

Starting 25 years ago, numerous studies have demonstrated that dietary MetR improves healthspan, lowers weight gain, and increases insulin sensitivity in mice, ultimately prolonging lifespan and resulting in decreased risk for cardiovascular disease^{3, 5, 18, 29, 30}. This is typically associated with decreased adiposity and improved metabolic measures, a reduction in mitochondrial oxidative stress, changes in cellular proliferation or apoptosis, and potential changes in epigenetic regulation. Recent studies of MetR^{31, 32} showed that MetR is sufficient to reduce body mass and adiposity even in mice fed a high-fat diet, independently of FGF21 or adiponectin, and our study reflects these expectations. In addition, WAT undergoes changes in apoptosis, chaperone-mediated autophagy, and macroautophagy as mechanisms of adipose tissue remodeling³¹. Furthermore, MetR reduced inflammation in WAT, which was also independent of FGF21 activity³². In rats, dietary MetR also increased UCP1 expression in BAT and WAT³³.

Initiation of dietary MetR in young, growing animals has been reported to produce temporal responses in body composition that are sexually dimorphic¹⁵. Forney et al. studied mice on 0.17% MetR diet and observed males preserving lean tissue at the expense of fat and females preserving fat at the expense of lean tissue. In young females, the increase in energy expenditure develops slower than in age-matched males. Despite these differences in rates of increased energy expenditure, all responses to MetR, such as decreases in body weight, lean mass, and fat mass accumulation, were similar between the sexes after 8 weeks on MetR diet. The differences in energy balance between females and males were only observed when MetR was initiated in young mice (MetR started at 8-weeks) and were attributed to a difference in nutrient partitioning from the female having greater energy demands to support reproduction. The effects of MetR on energy balance in males and females were comparable when the diet was initiated after attainment of maturity and full body size (MetR started at 3-months). Since weight loss was primarily adipose tissue in both sexes and interestingly the transcriptional responses across target tissues were similarly significantly expressed between control and MetR diets (liver- *Fgf21*, *Asns*, *Psat1*, *Scd1*; BAT- *Bmp8b*, *Ucp1*; iWAT- *Cox7a*, *Fatp2*, *Ucp1* and *Lep*), there is little evidence for sex-specific molecular responses to the diet. Our current study focused on male mice because MetR initiated in young male mice lead to loss of overall fat mass, which does not occur consistently in young female mice, and MetR-induced changes in weight loss and energy balance are comparable between the sexes over time. Our rationale for focusing on the young age group for thermogenic activation in PVAT and adipose depots is that young mice have been reported to have the most robust response to MetR diets in terms of weight loss.

We are not aware of publications analyzing PVAT as a result of dietary MetR, however a related abstract has examined effects of MetR on control or high-fat diet in the rat⁹. Because the main focus of that prior rat study was vascular reactivity and the anti-contractile function of PVAT, the thermogenic phenotype was not studied, and the mesenteric arteries and associated PVAT were the depot of interest. While the PVAT of the mesenteric arteries is known to be mostly WAT, this study did not examine effects of MetR diet on thermogenic properties. Our study focused on PVAT surrounding the thoracic aorta because it is thermogenic in nature, and can expand into more of a white adipocyte phenotype with robust lipid storage (induced by high-fat diet), but also lose considerable lipid and adopt an enhanced thermogenic phenotype (induced by calorie restriction)²². We demonstrated that MetR prevents age-related weight gain and lipid accumulation in PVAT from the thoracic aorta, while improving physiological health at three different age phases in the mouse: mature young adult, middle-aged adult, and old adult. This included at all ages a decrease in lipid accumulation within the aortic PVAT. In addition, the presence of thermogenic adipocyte markers was enhanced in mature mice after one year of MetR diet, but not increased in middle-aged mice, which did not start dietary modification until one year of age. These data show that while lipid content of PVAT correlated with body weight and markers of metabolic health, expression of thermogenic markers increased in the young cohort in PVAT, but not in the middle aged-cohort. Our study identified the largest effects of MetR when initiated in young adult mice. Because there are known phenotypic differences in PVAT based on anatomical location, our findings are limited to PVAT of thoracic aorta.

Methionine, as the precursor to homocysteine, has been shown using methionine-rich diets to be related to cardiovascular pathology, and local PVAT-derived paracrine effects are relevant since PVAT is localized within the vascular microenvironment. Our study provides the first analysis of PVAT responses with MetR, examining different aged cohorts. Our findings show that there are several conserved features of the PVAT response. Regardless of the initiating age for a one-year long MetR diet (8 weeks vs 1 year old starting age), the ending lipid storage phenotype of the PVAT was similar. Even initiation of MetR diet in 102 week old mice for a shorter 15 week duration reverted the PVAT to a similar, lower lipid state. However, differences in timing of initiation of the MetR diet affected the molecular thermogenic phenotype. With early initiation of MetR diet (8 weeks of age), the young cohort had elevation of thermogenic adipocyte markers UCP1, CoxIV, and GRP75 in PVAT, whereas this was not observed in the middle-aged cohort initiation of MetR diet at one year of age. While limiting amounts of mouse PVAT tissue make it more difficult to define regulators of mitochondrial respiration and relationship to lipid accumulation, mouse PVAT surrounding the thoracic aorta phenotypically resembles mouse interscapular BAT. In mouse BAT, recent studies have shown that this depot has a mixture of populations that represent either high- or low-thermogenic phenotypes³⁴, which can adopt high-thermogenic capacity with cold stimulation. Interestingly, in their study, this cold responsiveness is blunted with age, decreasing as early as 30 weeks of age and also at 60 weeks of age. In our study analyzing PVAT, the loss of stimulation of thermogenic markers by MetR in middle-aged mice is consistent with this concept that aging blunts responsiveness to stimuli that increase thermogenesis in younger mice.

In mouse PVAT, activation of the thermogenic phenotype has been established by cold exposure. The function impact of this activation on cardiovascular disease was previously shown using an ApoE null high-fat diet atherogenesis model⁸. This study showed that cold-activation of atherosusceptible mice increased thermogenic adipocyte markers in PVAT and significantly decreased lesion area. Similarly, we expect that other activators of PVAT thermogenesis, including MetR may likewise be protective against vascular disease. Cellular mechanisms downstream of thermogenic activation of PVAT include increased mitochondrial activity, activated thermogenic genes, secretion of batokines (originally defined as BAT-secreted factors that improve metabolic efficiency³⁵), and suppression of immune-related factors, all of which have the capacity to impact vascular disease^{36–40}. Mechanisms of MetR in PVAT phenotype and impact on vascular disease are currently critical areas of study. In addition to well-known activation of thermogenesis by cold and adrenergic stimulation, circadian disruption has also been linked to altered thermogenic gene expression in PVAT⁴¹. Our studies define the temporal and age-related changes in PVAT induced by dietary MetR as another regulation of PVAT physiology.

We predict that the PVAT phenotype induced especially by early initiation of MetR may protect from obesity-related vascular dysfunction and be associated with suppression of age-related cardiovascular disease. Additional research is needed that to address the effects on MetR on PVAT in the vascular microenvironment, and mechanisms that regulate the relationship of MetR in adiposity. In addition, it is important to determine how phenotypes seen in model organisms such as the mouse pertain to human PVAT, particularly in cardiovascular disease. Our recent collaborative work⁴² studying the lineage of PVAT

has indicated that there are some similarities in mouse PVAT-derived adipose progenitor cells and human PVAT-derived adipose progenitor cells, but that human PVAT has unique characteristics that will be important to continue to define at a molecular levels. Our results in the mouse have significance in understanding how dietary changes can impact adipose tissue within the vascular microenvironment.

Supplementary Material

Refer to Web version on PubMed Central for supplementary material.

Acknowledgements

The authors thank Armie Mangoba and Dr. Volkhard Lindner from the Histopathology Core Facility at MaineHealth Institute for Research for tissue processing and histology and advice with antibody characterization for immunostaining procedures.

Sources of funding -

This study was supported by NIH/NHLBI grant R01 HL141149 to LL and American Heart Association grant 19TPA34850041 to LL. Our institutional Histopathology core facility is supported by NIH/NIGMS award 1P20GM12130 to LL and NIH/NIGMS award U54GM115516 (C. Rosen and G. Stein, PIs).

References

1. Benjamin EJ, Blaha MJ, Chiuve SE, Cushman M, Das SR, Deo R, Ferranti SD, Floyd J, Fornage M, Gillespie C, Isasi CR, Jiménez MC, Jordan LC, Judd SE, Lackland D, Lichtman JH, Lisabeth L, Liu S, Longenecker CT, Mackey RH, Matsushita K, Mozaffarian D, Mussolino ME, Nasir K, Neumar RW, Palaniappan L, Pandey DK, Thiagarajan RR, Reeves MJ, Ritchey M, Rodriguez CJ, Roth GA, Rosamond WD, Sasson C, Towfighi A, Tsao CW, Turner MB, Virani SS, Voeks JH, Willey JZ, Wilkins JT, Wu JH, Alger HM, Wong SS, Muntner P, Subcommittee AHASCaSS. Heart disease and stroke statistics;2017 update: A report from the american heart association. *Circulation*. 2017;135:e146–e603 [PubMed: 28122885]
2. Ables GP, Hens JR, Nichenametla SN. Methionine restriction beyond life-span extension. *Ann N Y Acad Sci*. 2016;1363:68–79 [PubMed: 26916321]
3. Ables GP, Johnson JE. Pleiotropic responses to methionine restriction. *Exp Gerontol*. 2017;94:83–88 [PubMed: 28108330]
4. Richie JP Jr., Leutzinger Y Fau - Parthasarathy S, Parthasarathy S Fau - Malloy V, Malloy V Fau - Orentreich N, Orentreich N Fau - Zimmerman JA, Zimmerman JA. Methionine restriction increases blood glutathione and longevity in f344 rats. *FASEB*. 1994 Dec;8:1302–1307
5. Miller RA, Buehner G Fau - Chang Y, Chang Y Fau - Harper JM, Harper Jm Fau - Sigler R, Sigler R Fau - Smith-Wheelock M, Smith-Wheelock M. Methionine-deficient diet extends mouse lifespan, slows immune and lens aging, alters glucose, t4, igf-i and insulin levels, and increases hepatocyte mif levels and stress resistance. 2005 Jun;4:119–125
6. Sanchez-Roman I, Barja G. Regulation of longevity and oxidative stress by nutritional interventions: Role of methionine restriction. *Experimental Gerontology*. 2013 Oct;48:1030–1042 [PubMed: 23454735]
7. Chang L, Garcia-Barrio MT, Chen YE. Perivascular adipose tissue regulates vascular function by targeting vascular smooth muscle cells. *Arterioscler Thromb Vasc Biol*. 2020;40:1094–1109 [PubMed: 32188271]
8. Chang L, Villacorta L, Li R, Hamblin M, Xu W, Dou C, Zhang J, Wu J, Zeng R, Chen YE. Loss of perivascular adipose tissue upon peroxisome proliferator-activated receptor-gamma deletion in smooth muscle cells impairs intravascular thermoregulation and enhances atherosclerosis. *Circulation*. 2012;126:1067–1078 [PubMed: 22855570]

9. Lee D, Corken A, Wahl EC, Thakali KM. Does dietary methionine alter perivascular adipose tissue function? *The FASEB Journal*. 2022;36
10. Brown NK, Zhou Z, Zhang J, Zeng R, Wu J, Eitzman DT, Chen YE, Chang L. Perivascular adipose tissue in vascular function and disease: A review of current research and animal models. *Arterioscler Thromb Vasc Biol*. 2014;34:1621–1630 [PubMed: 24833795]
11. Fitzgibbons TP, Kogan S Fau - Aouadi M, Aouadi M Fau - Hendricks GM, Hendricks Gm Fau - Straubhaar J, Straubhaar J Fau - Czech MP, Czech MP. Similarity of mouse perivascular and brown adipose tissues and their resistance to diet-induced inflammation. *American Journal of Physiology Heart and Circulatory Physiology*. 2011;301:H1425–1437 [PubMed: 21765057]
12. Boucher JM, Ryzhova L, Harrington A, Davis-Knowlton J, Turner JE, Cooper E, Maridas D, Ryzhov S, Rosen CJ, Vary CPH, Liaw L. Pathological conversion of mouse perivascular adipose tissue by notch activation. *Arteriosclerosis, Thrombosis, and Vascular Biology*. 2020;40:2227–2243 [PubMed: 32640901]
13. Kaisanlahti A, Glumoff T. Browning of white fat: Agents and implications for beige adipose tissue to type 2 diabetes. *J Physiol Biochem*. 2019;75:1–10 [PubMed: 30506389]
14. Ikeda K, Maretich P, Kajimura S. The common and distinct features of brown and beige adipocytes. *Trends Endocrinol Metab*. 2018;29:191–200 [PubMed: 29366777]
15. Forney LA, Stone KP, Gibson AN, Vick AM, Sims LC, Fang H, Gettys TW. Sexually dimorphic effects of dietary methionine restriction are dependent on age when the diet is introduced. *Obesity (Silver Spring)*. 2020;28:581–589 [PubMed: 32012481]
16. Tero BW, Fortier B, Soucy AN, Paquette G, Liaw L. Quantification of lipid area within thermogenic mouse perivascular adipose tissue using standardized image analysis in fiji. *J Vasc Res*. 2022;59:43–49 [PubMed: 34736260]
17. Lees EK, Król E Fau - Grant L, Grant L Fau - Shearer K, Shearer K Fau - Wyse C, Wyse C Fau - Moncur E, Moncur E Fau - Bykowska AS, Bykowska As Fau - Mody N, Mody N Fau - Gettys TW, Gettys Tw Fau - Delibegovic M, Delibegovic M. Methionine restriction restores a younger metabolic phenotype in adult mice with alterations in fibroblast growth factor 21. *Aging Cell*. 2014;13:817–827 [PubMed: 24935677]
18. Malloy VL, Krajcik Ra Fau - Bailey SJ, Bailey Sj Fau - Hristopoulos G, Hristopoulos G Fau - Plummer JD, Plummer Jd Fau - Orentreich N, Orentreich N. Methionine restriction decreases visceral fat mass and preserves insulin action in aging male fischer 344 rats independent of energy restriction. *Aging Cell*. 2006 Aug;5:305–314 [PubMed: 16800846]
19. Lees EK, Krol E, Shearer K, Mody N, Gettys TW, Delibegovic M. Effects of hepatic protein tyrosine phosphatase 1b and methionine restriction on hepatic and whole-body glucose and lipid metabolism in mice. *Metabolism*. 2015;64:304–314
20. Wanders D, Stone KP, Forney LA, Cortez CC, Dille KN, Simon J, Xu M, Hotard EC, Nikonorova IA, Pettit AP, Anthony TG, Gettys TW. Role of *gcn2*-independent signaling through a noncanonical *perk/nrf2* pathway in the physiological responses to dietary methionine restriction. *Diabetes*. 2016 Jun;65:1499–1510 [PubMed: 26936965]
21. Ghosh S, Wanders D, Stone KP, Van NT, Cortez CC, Gettys TW. A systems biology analysis of the unique and overlapping transcriptional responses to caloric restriction and dietary methionine restriction in rats. *FASEB J*. 2014 Jun;28:2577–2590 [PubMed: 24571921]
22. Boucher JM, Ryzhova L, Harrington A, Davis-Knowlton J, Turner JE, Cooper E, Maridas D, Ryzhov S, Rosen CJ, Vary CPH, Liaw L. Pathological conversion of mouse perivascular adipose tissue by notch activation. *Arterioscler Thromb Vasc Biol*. 2020;40:2227–2243 [PubMed: 32640901]
23. Patil YN, Dille KN, Burk DH, Cortez CC, Gettys TW. Cellular and molecular remodeling of inguinal adipose tissue mitochondria by dietary methionine restriction. *Journal of Nutritional Biochemistry*. 2015;26:1235–1247 [PubMed: 26278039]
24. Moseti D, Regassa A, Kim WK. Molecular regulation of adipogenesis and potential anti-adipogenic bioactive molecules. *Lid - 10.3390/ijms17010124 [doi] lid - 124*.
25. Tang QQ, Lane MD. Adipogenesis: From stem cell to adipocyte. *Annual Review of Biochemistry*. 2012;81:715–736

26. Brasaemle DL. Thematic review series: Adipocyte biology. The perilipin family of structural lipid droplet proteins: Stabilization of lipid droplets and control of lipolysis. *Journal of Lipid Research*. 2007;48:2547–2559 [PubMed: 17878492]
27. Furuhashi M Fatty acid-binding protein 4 in cardiovascular and metabolic diseases. *J Atheroscler Thromb*. 2019;26:216–232 [PubMed: 30726793]
28. Zheng C, Yang Q, Xu C, Shou PA-O, Cao J, Jiang M, Chen Q, Cao G, Han Y, Li F, Cao W, Zhang L, Zhang L, Shi Y, Wang Y. Cd11b regulates obesity-induced insulin resistance via limiting alternative activation and proliferation of adipose tissue macrophages. *Proceedings of the National Academy of Sciences of the United States*. 2015;112:E7239–7248
29. Perrone CE, Malloy VI, Orentreich DS, Orentreich N. Metabolic adaptations to methionine restriction that benefit health and lifespan in rodents. *Experimental Gerontology*. 2013;48:654–660 [PubMed: 22819757]
30. Ables GP, Perrone CE, Orentreich D, Orentreich N. Methionine-restricted c57bl/6j mice are resistant to diet-induced obesity and insulin resistance but have low bone density. *PLoS One*. 2012;7:e51357 [PubMed: 23236485]
31. Cooke D, Mattocks D, Nichenametla SN, Anunciado-Koza RP, Koza RA, Ables GP. Weight loss and concomitant adipose autophagy in methionine-restricted obese mice is not dependent on adiponectin or fgf21. *Obesity (Silver Spring)*. 2020;28:1075–1085 [PubMed: 32348021]
32. Sharma S, Dixon T, Jung S, Graff EC, Forney LA, Gettys TW, Wanders D. Dietary methionine restriction reduces inflammation independent of fgf21 action. *Obesity (Silver Spring)*. 2019;27:1305–1313 [PubMed: 31207147]
33. Hasek BE, Stewart LK, Henagan TM, Boudreau A, Lenard NR, Black C, Shin J, Huypens P, Malloy VL, Plaisance EP, Krajcik RA, Orentreich N, Gettys TW. Dietary methionine restriction enhances metabolic flexibility and increases uncoupled respiration in both fed and fasted states. *Am J Physiol Regul Integr Comp Physiol*. 2010;299:R728–739 [PubMed: 20538896]
34. Song A, Dai W, Jang MJ, Medrano L, Li Z, Zhao H, Shao M, Tan J, Li A, Ning T, Miller MM, Armstrong B, Huss JM, Zhu Y, Liu Y, Gradinaru V, Wu X, Jiang L, Scherer PE, Wang QA. Low- and high-thermogenic brown adipocyte subpopulations coexist in murine adipose tissue. *J Clin Invest*. 2020;130:247–257 [PubMed: 31573981]
35. Nishio M, Saeki K. The remaining mysteries about brown adipose tissues. *Cells*. 2020;9
36. Mestres-Arenas A, Villarroya J, Giralt M, Villarroya F, Peyrou M. A differential pattern of batokine expression in perivascular adipose tissue depots from mice. *Front Physiol*. 2021;12:714530 [PubMed: 34421656]
37. Reynés B, van Schothorst EM, Keijer J, Ceresi E, Oliver P, Palou A. Cold induced depot-specific browning in ferret aortic perivascular adipose tissue. *Front Physiol*. 2019;10:1171 [PubMed: 31620014]
38. Reynés B, van Schothorst EM, García-Ruiz E, Keijer J, Palou A, Oliver P. Cold exposure down-regulates immune response pathways in ferret aortic perivascular adipose tissue. *Thromb Haemost*. 2017;117:981–991 [PubMed: 28251235]
39. Koenen M, Hill MA, Cohen P, Sowers JR. Obesity, adipose tissue and vascular dysfunction. *Circ Res*. 2021;128:951–968 [PubMed: 33793327]
40. Kim HW, Shi H, Winkler MA, Lee R, Weintraub NL. Perivascular adipose tissue and vascular perturbation/atherosclerosis. *Arterioscler Thromb Vasc Biol*. 2020;40:2569–2576 [PubMed: 32878476]
41. Pati P, Valcin JA, Zhang D, Neder TH, Millender-Swain T, Allan JM, Sedaka R, Jin C, Becker BK, Pollock DM, Bailey SM, Pollock JS. Liver circadian clock disruption alters perivascular adipose tissue gene expression and aortic function in mice. *Am J Physiol Regul Integr Comp Physiol*. 2021;320:R960–r971 [PubMed: 33881363]
42. Angueira AR, Sakers AP, Holman CD, Cheng L, Arbocco MN, Shamsi F, Lynes MD, Shrestha R, Okada C, Batmanov K, Susztak K, Tseng YH, Liaw L, Seale P. Defining the lineage of thermogenic perivascular adipose tissue. *Nat Metab*. 2021;3:469–484 [PubMed: 33846639]

- Dietary methionine restriction is known in multiple organisms to lead to increased lifespan, reduced adiposity, and overall metabolic health.
- The phenotype and thermogenic characteristics of perivascular adipose tissue regulate cardiovascular health.
- Our study provides novel analysis of thermogenic adipocytes, in particular perivascular adipose tissue, which has not previously been studied in this context. We analyze novel thermogenic targets in multiple adipose tissues.
- In this mouse model of normal aging with dietary methionine restriction, we find unique responses in different adipose tissues and based on age of onset of methionine restriction.
- Perivascular adipose tissue, as well as more classically studied visceral white adipose tissue, is an important target that will affect metabolic health, comorbidities, and disease.

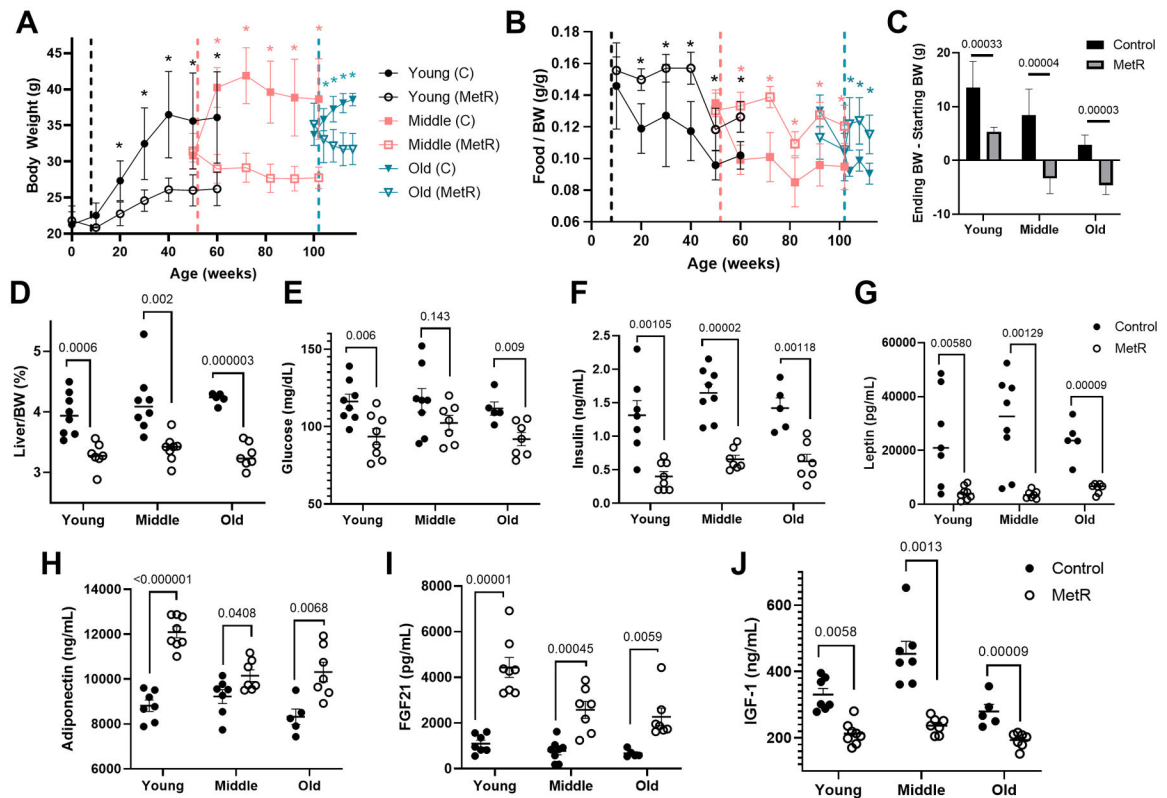


Figure 1. Dietary methionine restriction promotes metabolic health at all ages.

A) Body weights of C57BL/6J male mice fed a control or MetR diet over a 52 (young and middle aged groups n=8/diet/age) or 15 week period (old group, n=5 control and n=8 MetR). Significant comparisons are depicted with asterisks, color corresponds to age group. B) Food consumption expressed as grams of food consumed / grams of body weight, indicating reduction in body weight is not a direct response to decreased caloric intake. C) Change in body weight over the course of the dietary treatment is shown. D) Liver weight divided by body weight, represented as a percentage. Comparisons of endpoint levels of glucose (E), insulin ng/mL (F) leptin, pg/mL (G), adiponectin, ng/mL (H), fibroblast growth factor – 21 (FGF21), pg/mL (I), and insulin-like growth factor (IGF1), ng/mL (J). Graphed are means \pm SEM, and differences evaluated by students t test (p values indicated).

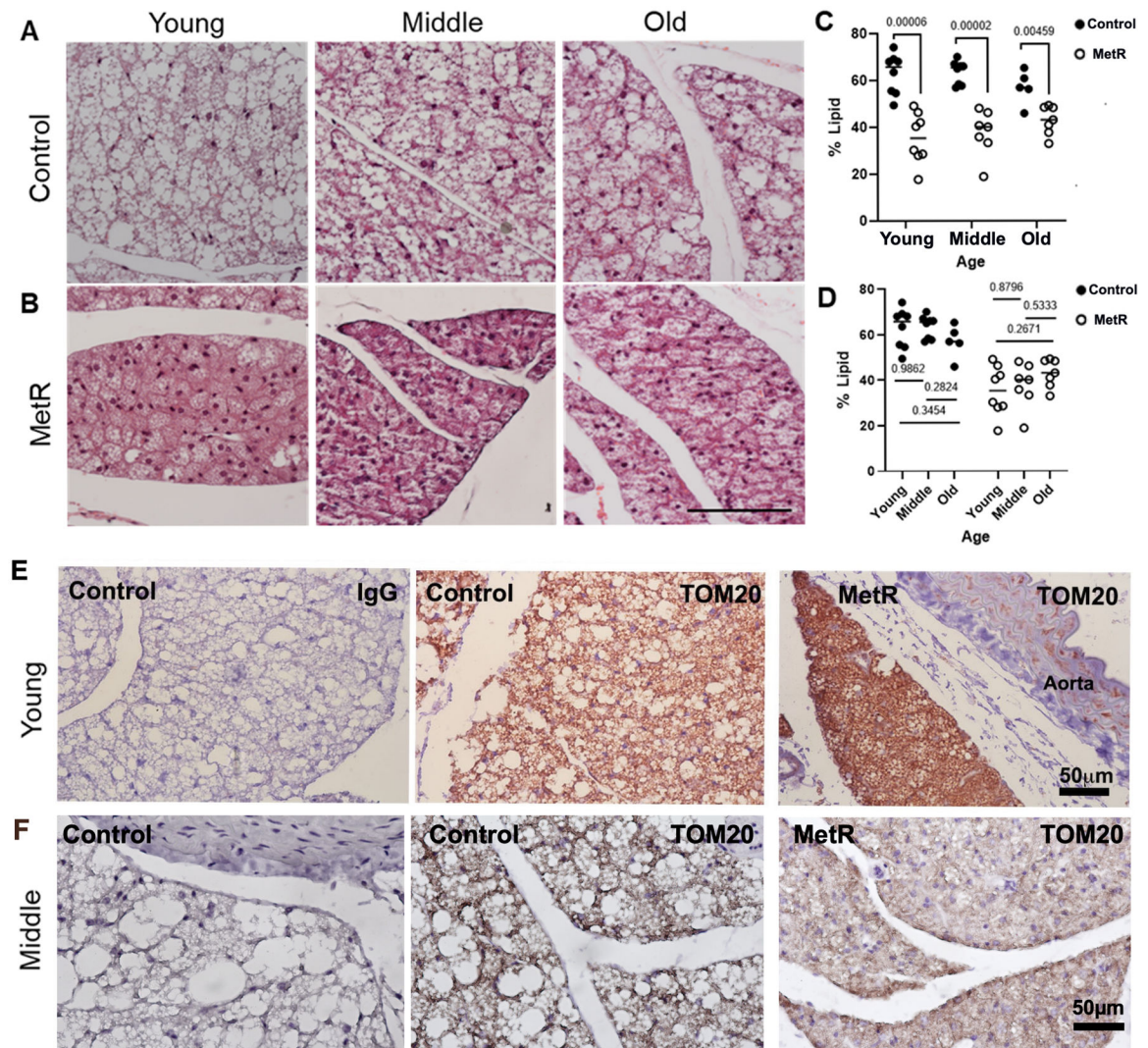


Figure 2. Dietary MetR prevents lipid accumulation in mouse PVAT and increases a mitochondrial marker.

A) Representative H&E stains show PVAT morphology in control versus **B)** MetR mice for the different cohorts of mice. Scale bar (100µm) represents all images. **C-D)** The relative amount of lipid region in the PVAT was quantified. **C)** Diet group comparisons. **D)** Age group comparisons. Values graphed are means \pm SEM, and statistical analysis was performed with students t-tests. ns=not significant. For young and middle aged cohorts, n=8/diet/age; for Old cohort, n= n=5 control and n=8 MetR. **E)** PVAT sections from the young cohort at 60 weeks of age or middle-aged cohort at 104 weeks of age were immunostained to detect the mitochondrial marker TOM20. Scale bar =50µm.

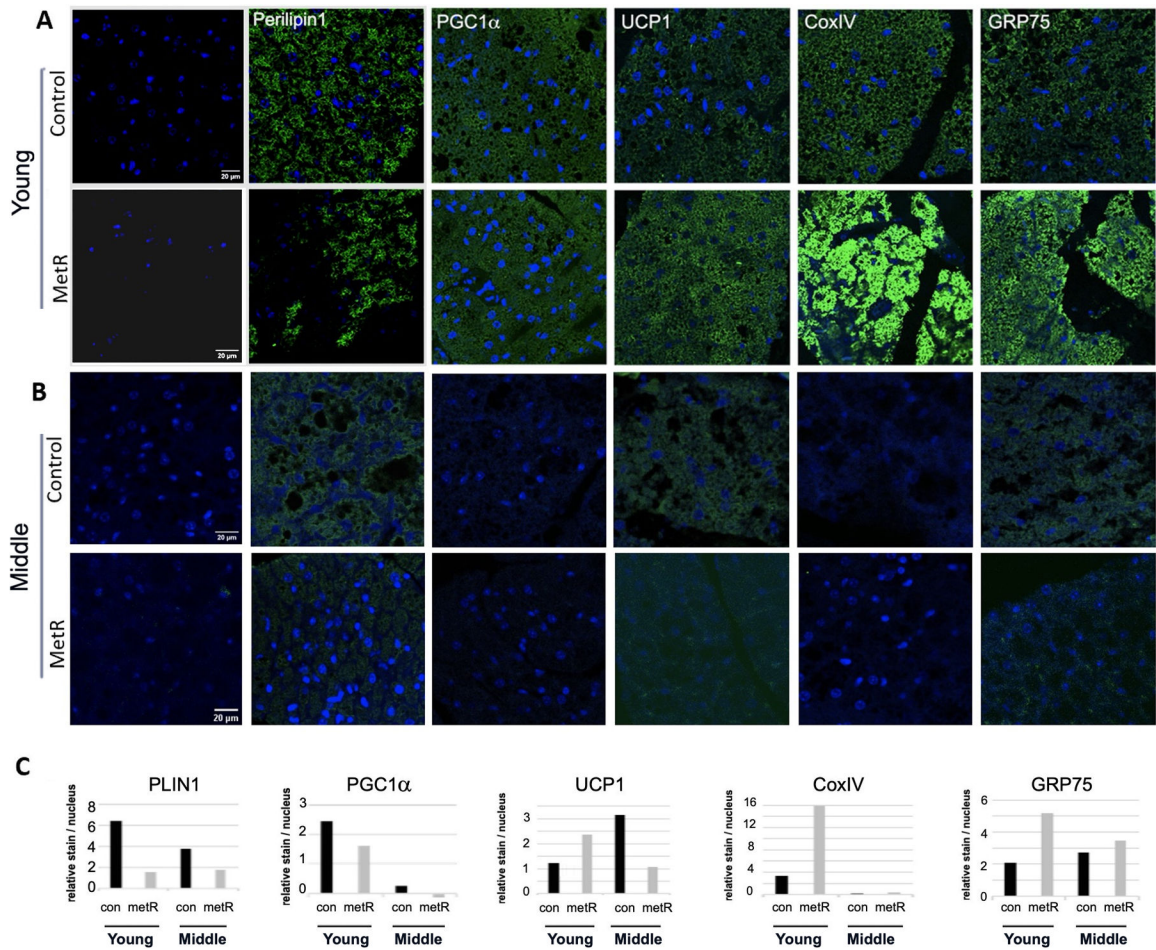


Figure 3. Early initiation of dietary MetR affects thermogenic phenotype of PVAT.

A-B) Immunofluorescence staining of adipocyte and thermogenic markers. Representative images of PVAT of mice from the young cohort at 60 weeks of age (A), and from the middle aged cohort at 104 weeks of age. **C)** Quantification of fluorescence, y-axis is normalized relative abundance (raw density of fluorescence divided by number of DAPI stained nuclei). Far left image is control IgG image in which relative abundance of specific antigens were normalized. Scale bar =20 μ m.

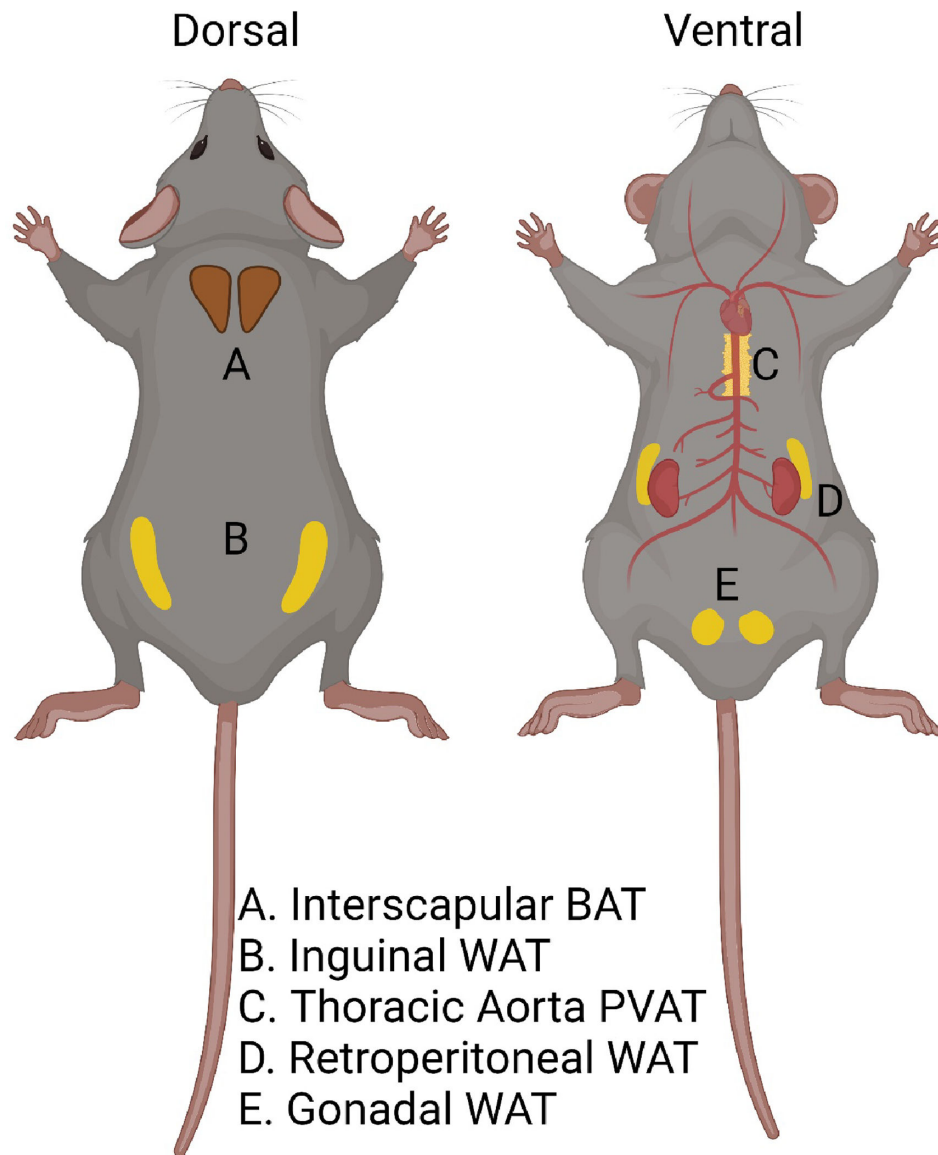


Figure 4. Anatomical distinction of adipose depots.

Locations of adipose tissues collected for this study are shown. These include (left) subcutaneous brown adipose tissue (A) and inguinal white adipose tissue (B), and (right) perivascular adipose tissue around the thoracic aorta (C), retroperitoneal white adipose tissue (D), and gonadal white adipose tissue (E). Created with [Biorender.com](https://biorender.com)

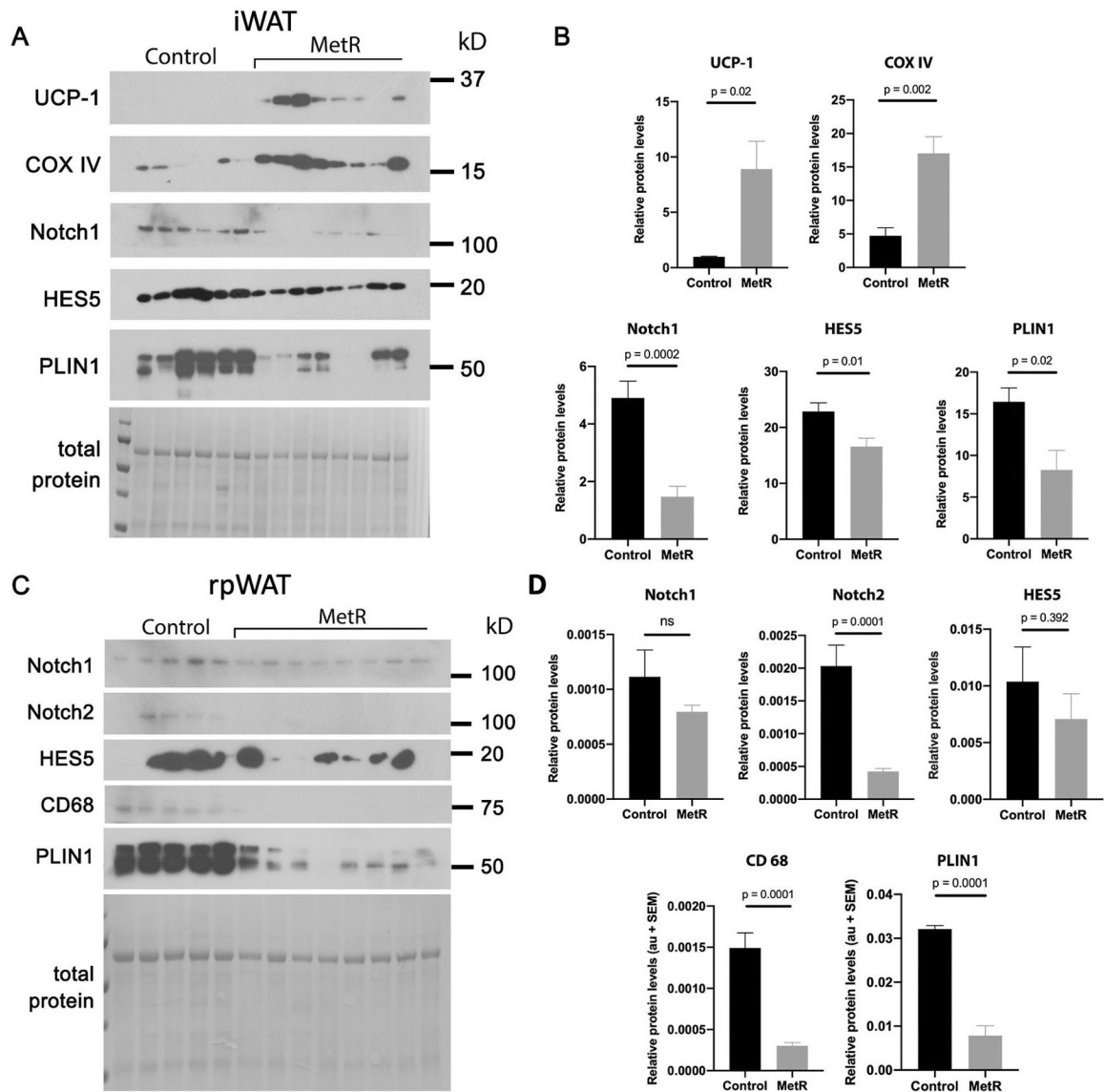


Figure 5. Early initiation of dietary MetR in young mice affects white adipose depots with capacity to beige.

Immunoblot analysis was used to quantify thermogenic markers and Notch signaling components in the young cohort from tissues collected at 60 weeks of age from **A-B**) inguinal white adipose tissue (iWAT) or **C-D**) retroperitoneal white adipose tissue (rpWAT) derived from control or MetR mice (n=8/group). Band intensities were normalized to total protein and represented as relative difference between experimental groups. Graphed are means \pm SEM, with p values indicated, ns = not significant.

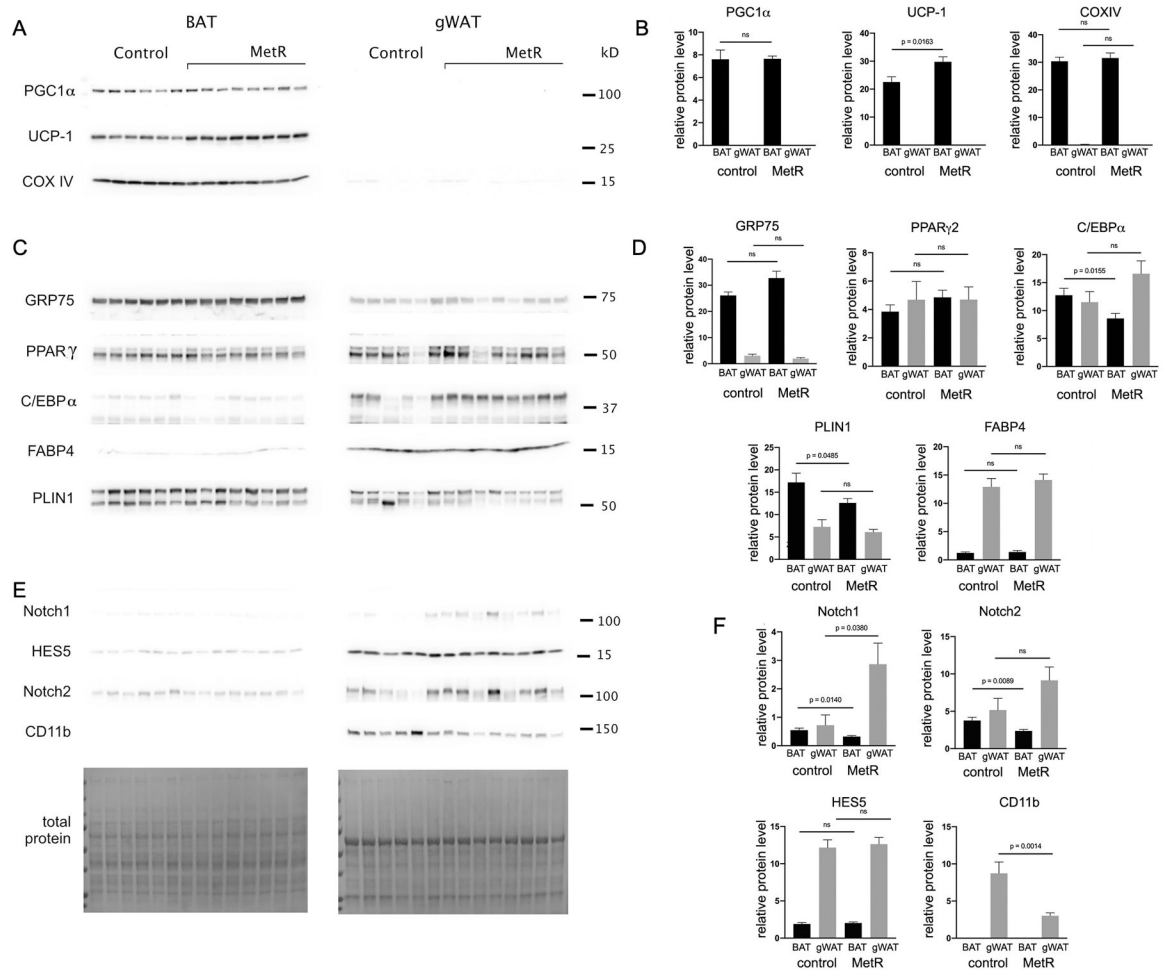


Figure 6. Adipose depot-specific effects of dietary MetR.
A, C, E) Immunoblot analysis was performed using BAT and gWAT from the young cohort fed control or MetR diet for one year (n=8/diet). Representative samples from each experimental group are shown. Band signals were normalized to total protein, and relative differences for each adipose tissue and each protein are shown in **B, D, F**). Graphed are means \pm SEM. P values for comparisons are shown for groups values that were significantly different, ns = not significant.